esa

ECOSPHERE

SPECIAL FEATURE: DATA ASSIMILATION

Improving the quantification of terrestrial ecosystem carbon dynamics over the United States using an adjoint method

QING ZHU[1,†] AND QIANLAI ZHUANG[1,2]

[1]*Department of Earth, Atmospheric and Planetary Sciences, Purdue University, West Lafayette, Indiana 47906 USA*
[2]*Department of Agronomy, Purdue University, West Lafayette, Indiana 47906 USA*

Citation: Zhu, Q., and Q. Zhuang. 2013. Improving the quantification of terrestrial ecosystem carbon dynamics over the United States using an adjoint method. Ecosphere 4(10):118. http://dx.doi.org/10.1890/ES13-00058.1

Abstract. We used an adjoint version of the process-based Terrestrial Ecosystem Model (TEM) to optimize the model parameters in a spatially explicit manner by assimilating satellite-based estimates of gross primary production (GPP) in the conterminous United States. Traditionally, terrestrial ecosystem model parameterization is conducted at site-level for various plant functional types (PFTs). The optimal parameters are then extrapolated to regions that have the same plant functional types as parameterized. However, site-level parameterization might be only valid within a few kilometers in the footprint of the individual site. Extrapolation of the optimal parameters to a region with an assumption that the parameters are the same for all pixels for the same ecosystem type in the region may introduce significant errors in quantification of regional carbon dynamics. This study used Moderate Resolution Imaging Spectroradiometer GPP to optimize parameters for each pixel using adjoint method in a spatially explicit manner. The spatially explicit parameters were then used to quantify the regional carbon fluxes from 2000 to 2005. The estimated net ecosystem production (NEP) was used to drive a global atmospheric transport model, GEOS-Chem, to estimate the near surface atmospheric CO_2 concentrations, which were then compared with flask measurements. We found that (1) the site-level TEM parameterization method provided good estimates of carbon fluxes at site levels, but had a large uncertainty in the regional simulations; (2) the spatially explicit parameterization improved the estimates of the spatial distribution and seasonal variation of regional carbon dynamics; and (3) when driven with the NEP estimated with the spatially explicit model, the GEOS-Chem captured the seasonal trend of near-surface CO_2 concentrations better than that was driven with the estimates based on the site-level parameterized model. This study suggested that future quantification of regional carbon dynamics should consider the spatial variation of parameters, which could be optimized using spatially explicit carbon flux data.

Key words: adjoint method; spatially explicit parameterization; Special Feature: Data Assimilation; Terrestrial Ecosystem Modeling; United States carbon dynamics.

Received 15 February 2013; revised 17 July 2013; accepted 18 July 2013; final version received 6 September 2013; **published** 7 October 2013. Corresponding Editor: Y. Luo.

† **E-mail:** zhuq@purdue.edu

INTRODUCTION

Atmospheric CO_2 has increased significantly since pre-industrial times due to human activities such as fossil fuel emissions and land-use and land-cover changes (Forster et al. 2007). There has been great progress in the understanding of spatial distribution and temporal evolution of

natural and anthropogenic CO_2 sources and sinks on regional and global scales (Yevich and Logan, 2003, van der Werf et al. 2006, Takahashi et al. 2009, Andres et al. 2011). However, the existing quantification of the sink and source activities and the ecosystem models still has great uncertainties. To date, two major techniques including atmospheric inverse modeling (top-down approach) and biogeochemical modeling (bottom-up approach) are used to estimate the net carbon exchanges between the atmosphere and terrestrial ecosystems. The top-down approach uses atmospheric transport and chemistry models and observed atmospheric CO_2 concentration data to estimate the regional carbon fluxes (e.g., Kaminski et al. 1999*a*, Kaminski et al. 1999*b*, Gurney et al. 2002, Kaminski et al. 2002, Law et al. 2008). This approach can hardly reveal insights of the ecosystem processes at high temporal and spatial resolutions, thus limit its prognostic capability in predicting terrestrial carbon fluxes. In contrast, bottom-up biogeochemical models have been widely used for modeling ecosystem processes and carbon and nitrogen dynamics (e.g., Running and Coughlan 1988, Raich et al. 1991, McGuire et al. 1992, Melillo et al. 1993, Filed et al. 1995, Luo et al. 2003, Zhuang et al. 2003, Wang et al. 2009). However, model sensitivity and uncertainty studies have shown that estimations of carbon fluxes using biogeochemical models are also of a large uncertainty due to uncertain model structure, parameterization, and forcing data (e.g., Tang and Zhuang 2008, Tang and Zhuang 2009), in particular, the accuracy of model parameters is an important source of uncertainty (Zaehle et al. 2005, Alton et al. 2007).

To this end, data assimilation (DA) is an effective tool to improve ecosystem model parameter estimation and quantify model uncertainty (Raupach et al. 2005, Luo et al. 2011). Various DA methods have been used extensively to improve the model predictability. One group of methods is based on Monte Carlo simulation and Bayesian inference approaches (e.g., Braswell et al. 2005, Knorr and Kattge 2005, Xu et al. 2006, Ricciuto et al. 2008*a*, Ricciuto et al. 2008*b*, Tang and Zhuang 2008, Tang and Zhuang 2009). For example, Ricciuto et al. (2008*a*, 2008*b*) employed a Markov Chain Monte Carlo (MCMC) calibration technique to derive posterior probability density functions (PDFs) of model parameters, estimate the optimal values and uncertainties of the parameters that control carbon cycling. Kalman filter (KF) is another approach to calibrate model parameters and state variables by assimilating observational data (Kalman 1960). Different implementations of basic Kalman filter have been employed in ecosystem modeling studies. For example, the extended Kalman filter (EKF) (Carmillet et al. 2001, Hoteit et al. 2003) has been applied to data assimilation of non-linear marine biogeochemical models by linearizing the dynamic model operator and observation model operator. The ensemble Kalman filter (EnKF) (Evensen 1994, Reichle et al. 2002, Mo et al. 2008, Quaife et al. 2008, Gao et al. 2011) is a popular variant of basic KF. This method is favorable for complex ecosystem models that have a large number of variables to be optimized, since the error covariance matrix is approximated using ensemble model runs rather than being explicitly calculated. Another commonly used DA technique is the adjoint method. Adjoint approaches have been well used in the area of numeric weather forecast data assimilation system (Cacuci 1981*a*, Cacuci 1981*b*), atmospheric transport modeling (Kaminski et al. 1999*a*, Kaminski et al. 1999*b*), and ocean general circulation modeling (Marotzke et al. 1999, Li and Wunsch 2003, Li and Wunsch 2004). It is a powerful tool that can efficiently calculate the sensitivity and estimate the parameters of ecosystem models (Rayner et al. 2005, Tjiputra et al. 2007, Senina et al. 2008, Tjiputra and Winguth 2008, Kuppel et al. 2012, Kato et al. 2013).

Current DA techniques have been mostly applied to site-level parameterization. Consequently, with improved parameters, the biogeochemical models work well at site levels. However, the site-level parameterizations may only work at the site or a small region ranging from hundred meters to a few kilometers (Schmid 1994, Baldocchi 2003). For regional simulations, a conventional way is to divide a region into grid cells, conduct parameterizations at representative sites for each plant functional type, and then apply the parameters according to PFTs to all grid cells (e.g., Running and Coughlan 1988, Raich et al. 1991, Parton et al. 1993, Potter et al. 1993). This approach does not account for

spatially-varied parameters for ecosystems due to the variation of their structure (Bondeau et al. 1999), stand ages (Gower et al. 1996, Pregitzer and Euskirchen 2004, Zaehle et al. 2006, He et al. 2012), and species leaf longevity (Kitajima et al. 1997). To consider these spatial heterogeneities in parameterization, assimilating spatially explicit data into model for each grid cell has been shown as a good approach. For example, Zhou et al. (2009) assimilated global soil organic carbon (SOC) data (Global Soil Data Task 2000) into the Carnegie-Ames-Stanford-Approach (CASA model) (Potter et al. 1993) to estimate the spatial pattern of soil respiration parameter Q10 at a 1° by 1° resolution. They demonstrated that the spatial heterogeneous Q10 parameterization could improve the quantification of global soil respiration. Zhou and Luo (2008) employed the Terrestrial Ecosystem Regional model (TECO-R) to simulate carbon uptake combining NPP increase data and carbon residence time. Specifically, they compared the modeled carbon uptake that assuming a uniform NPP increase with that using actual spatial pattern of NPP increase. Their study highlighted the importance of spatial pattern of NPP increase in modeling the regional carbon uptake. However, model parameters controlling the carbon residence time were not optimized in a fully spatially explicit manner. Chen and Zhuang (2012) utilized multiple databases of carbon pools and fluxes to advance TEM parameterization to a spatially explicit manner. However, the model parameters were calibrated based on annual observed carbon fluxes data. Thus, the optimal parameters might not be able to capture the seasonal dynamics of carbon fluxes. In this study, we make a step forward to assimilate monthly observations into an adjoint TEM to improve model parameterization in a spatially explicit manner so as to improve the quantification of seasonal carbon dynamics in the conterminous U.S. region.

The specific goal of this study is to improve quantification of the carbon dynamics of terrestrial ecosystems in the conterminous United States using different parameterization approaches. The regional simulations of carbon fluxes are further evaluated by combining both top-down and bottom-up approaches and flask measurements of atmospheric CO_2 data. Specifically, two parameterization methods are used: (1) Using site-level Ameriflux data (Baldocchi et al. 2004, Bond-Lamberty et al. 2005, Hagen et al. 2006, Urbanski et al. 2007, Sulman et al. 2009) to parameterize TEM for each PFT and extrapolate the optimal parameters to the region; (2) Using MODIS GPP product (Running et al. 2004, Zhao et al. 2005, Heinsch et al. 2006, Zhao et al. 2006, Mu et al. 2007) to parameterize TEM for each grid cell (0.5° by 0.5°) and use parameters to simulate the carbon budget over the conterminous U.S. Both methods are based on a well-developed adjoint version of TEM (Q. Zhu and Q. Zhuang, *unpublished manuscript*). To evaluate the goodness of the simulated NEP, we conducted two sets of GEOS-Chem CO_2 simulations (Suntharalingam et al. 2003, Suntharalingam et al. 2004, Suntharalingam et al. 2005, Nassar et al. 2010) to estimate the seasonal variation of surface atmospheric CO_2 concentrations, driven with NEP simulated with two parameterization methods. The modeled seasonality of surface CO_2 concentrations was compared with flask measurements at various locations in the conterminous U.S. (Herbert et al. 1986, Komhyr et al. 1989, Thoning 1989, Bakwin et al. 1995, Masarie and Tans 1995, Masarie et al. 2001, GLOBALVIEW-CO2 2012).

Methods

Terrestrial Ecosystem Model (TEM) and data

The Terrestrial Ecosystem Model (TEM) is a process-based biogeochemical model, first developed by Raich et al. (1991) and further improved on both physical and biogeochemical mechanisms (McGuire et al. 1992, Melillo et al. 1993, Zhuang et al. 2003). TEM is a large-scale model forced with spatially explicit data of climate including precipitation, air temperature and solar irradiance and data on elevation, soils, and PFTs. It has been used to quantify regional (e.g., Raich et al. 1991) and global (e.g., Melillo et al. 1993) terrestrial ecosystem carbon dynamics at a monthly time step. Carbon fluxes between ecosystems and the atmosphere are estimated in terms of GPP (gross primary productivity), NPP (net primary productivity, defined as the difference between GPP and autotrophic respiration) and NEP (net ecosystem productivity, defined as the difference between GPP and total ecosystem respiration, including both autotro-

Table 1. Description of AmeriFlux flux sites used for traditional site-level TEM parameterization.

Site	Vegetation type	Available data	Principal Investigator(s)	Source
Howland Forest Main	Temperate coniferous forest	1996–2004	Hollinger D. Y.	Hagen et al. 2006, Richardson et al. 2006
Harvard Forest	Temperate deciduous forest	1992–2006	Munger J. W.	Urbanski et al. 2004, van Gorsel et al. 2009
Vaira Ranch	Grassland	2001–2007	Baldocchi D. D.	Baldocchi et al. 2004, Baldocchi et al. 2005
Lost Creek	Shrub land	2001–2005	Bolstad P. Cook B. Desai A.	Yuan et al. 2007, Sulman et al. 2009
UCI_1850	Boreal forest	2002–2005	Goulden M. L.	Bond-Lamberty et al. 2005, Goulden et al. 2011

phic and heterotrophic respiration). TEM algorithms are based on the interactions among five pools, which are vegetation carbon (C_v), soil carbon (C_s), vegetation nitrogen (N_v), soil nitrogen (N_s) and soil available inorganic nitrogen (N_{av}). The interactions among these pools form a complex nonlinear system, describing the terrestrial ecosystem carbon and nitrogen dynamics and the C-N feedbacks (McGuire et al. 1992). The soil thermal dynamics module (Zhuang et al. 2001, Zhuang et al. 2002) was incorporated into TEM to account for the effects of soil thermal dynamics on carbon and nitrogen cycling (Zhuang et al. 2003).

In this study, seven types of data are used, including atmospheric CO_2 concentrations, based on the observations at Mauna Loa, Hawaii (Conway et al. 1994, Masarie and Tans 1995), precipitation, solar radiation and air temperature (New et al. 1999, New et al. 2000, Mitchell et al. 2002, New et al. 2002, Mitchell et al. 2004), soil texture, elevation and PFTs (Raich et al. 1991, Zhuang et al. 2003). Model calibration data are from the AmeriFlux network and Moderate Resolution Imaging Spactro-radiometer (MODIS) observation product. The AmeriFlux network observes high frequency surface carbon, water and energy fluxes (Baldocchi et al. 2001) and provides level-4 monthly aggregated GPP and NEP. Eddy flux techniques directly measure NEP and GPP is derived from the observed NEP by subtracting daytime total ecosystem respiration (RESP), which is extrapolated from nighttime observed RESP with a temperature response function (Reichstein et al. 2005). Five eddy flux sites with high quality of data are selected in this study, covering the major representative PFTs over the conterminous U.S. (Table 1). Specifically, Howland Forest main (45.20N, 68.74W) (Hagen et al. 2006, Richardson et al. 2006), Harvard Forest main (42.54 N, 72.17 W) (Urbanski et al. 2007, van Gorsel et al. 2009), Vaira Ranch (38.41 N, 120.95 W) (Baldocchi et al. 2004, Baldocchi et al. 2005), Lost Creek (46.08 N, 89.98 W) (Yuan et al. 2007, Sulman et al. 2009) and UCI_1850 (55.88 N, 98.48 W) (Bond-Lamberty et al. 2005, Goulden et al. 2011) are used to parameterize for temperate coniferous forest, temperate deciduous forest, grassland, shrub land, and boreal forest, respectively. The optimal parameters are extrapolated to the conterminous United States.

For site-level parameterization, we used both GPP and NEP data. Although GPP data is derived based on the NEP observations using an empirical model (Reichstein et al. 2005), our previous research indicated that GPP provided important constraints on model parameters. If only NEP data are used in calibration, TEM modeled GPP and ecosystem respiration could be both over- or under-estimated, while the simulated NEP is acceptable compared with observational NEP. By using both NEP and GPP, both photosynthesis and ecosystem respiration are constrained and TEM parameters are consequently improved (Tang and Zhuang 2009).

For spatially explicit model parameterization and verification, we used the MOD17 GPP product from 2000 to 2005. MOD17 (Monteith 1972, Running and Coughlan 1988) provides 8-day interval composite GPP estimates (Running et al. 2004, Zhao et al. 2005, Heinsch et al. 2006, Zhao et al. 2006, Mu et al. 2007). The MOD17 algorithm is an empirical relationship that uses the absorbed photosynthetically active radiation (APAR) to predict GPP, where APAR is an estimation based on MODIS remotely sensed

Table 2. Parameters involved in this study.

ID	Abbreviation	Definition	Units	Lower bound	Upper bound
1	C_{max}	Maximum rate of photosynthesis C	g m^{-2} mon^{-1}	50	1500
2	K_I	Half saturation constant for PAR used by plants	J cm^{-2} d^{-1}	20	600
3	K_C	Half saturation constant for $C0_2$-C uptake by plants	μ L L^{-1}	20	600
4	T_{max}	Maximum temperature for GPP	°C	25	35
5	T_{min}	Minimum temperature for GPP	°C	−12	−1
6	T_{opt}	Maximum optimum temperature for GPP	°C	15	25
7	ALEAF	Coefficient A to model the relative photosynthetic capacity of vegetation	None	0.1	1.0
8	BLEAF	Coefficient B to model the relative photosynthetic capacity of vegetation	None	0.1	1.0
9	CLEAF	Coefficient C to model the relative photosynthetic capacity of vegetation	None	0.0	0.5
10	MINLEAF	Minimum photosynthesis capacity of vegetation	None	0.2	0.8
11	N_{max}	Maximum rate of N uptake by vegetation	mg m^{-2} mon^{-1}	50	700
12	K_{n1}	Half saturation constant for N uptake by vegetation	g m^{-3}	0.5	10
13	RAQ10A0	Leading coefficient of the Q10 model for plant respiration	None	1.350	3.3633
14	RAQ10A1	First order coefficient of the Q10 model for plant respiration	$°C^{-1}$	−0.054577	−0.051183
15	RAQ10A2	Second order coefficient of the Q10 model for plant respiration	$°C^{-2}$	0.0022902	0.0024381
16	RAQ10A3	Third order coefficient of the Q10 model for plant respiration	$°C^{-3}$	−0.0000417	−0.0000397
17	KDC	Heterotrophic respiration rate at 0°C	g g^{-1} mon^{-1}	0.0005	0.007
18	RHQ10	Change in heterotrophic respiration rate due to 10°C temperature change	None	1	3
19	MOISTMAX	Maximum soil moisture content for heterotrophic respiration	%	80	100
20	MOISTMIN	Minimum soil moisture content for heterotrophic respiration	%	20	80
21	MOISTOPT	Optimum soil moisture content for heterotrophic respiration	%	0	20
22	N_{up}	Ratio between N immobilized and C respired	mg g^{-1}	5	100
23	K_{n2}	Half saturation constant for N uptake by organisms	g m^{-3}	0.5	1.0
24	CFALL	Proportion of vegetation carbon loss as litterfall monthly	g g^{-1} mon^{-1}	0.0001	0.015
25	NFALL	Proportion of vegetation nitrogen loss as litterfall monthly	g g^{-1} mon^{-1}	0.003	0.012
26	KRC	plant respiration rate at 0°C	g g^{-1} mon^{-1}	$10^{-7.5}$	$10^{-1.5}$

fraction of photosynthetically active radiation absorbed by vegetation (fPAR) (Knyazikhin et al. 1999). MOD17 makes the spatially explicit model parameterization possible because the MODIS-derived fPAR captures the spatial distribution of the unique characteristics of terrestrial ecosystems for each grid cell.

Site-level and spatially explicit parameterization

An adjoint version of TEM (Q. Zhu and Q. Zhuang, *unpublished manuscript*) has been developed based on the general rules of adjoint code construction (Giering and Kaminski 1998). The gradient of a target variable with respect to model parameters ($\nabla_p g$) could be calculated with:

$$\nabla_p g = \left(\frac{\partial g_1}{\partial p}\right)^T \cdot \ldots \cdot \left(\frac{\partial g_i}{\partial g_{i-1}}\right)^T \cdot \ldots \cdot \left(\frac{\partial g_n}{\partial g_{n-1}}\right)^T \quad (1)$$

where T refers to the transposition. Eq. 1 aggregates all the intermediate results of transposition of the Jacobian Matrix $(\partial g_i/\partial g_{i-1})^T$ (i starts from n to 1) to get the gradient of the TEM output g with respect to the model parameter p. The gradient from Adjoint-TEM was then used to estimate the decreasing direction of the cost function J (Eq. 2):

$$J = J_{\text{obs}} + J_{\text{prior}} \quad (2)$$

$$J_{\text{obs}} = \sum_{i=1}^{N} (F_i(x) - y_i)^T R^{-1} (F_i(x) - y_i) \quad (3)$$

$$J_{\text{prior}} = \sum_{i=1}^{26} \frac{1}{8} \left[\frac{1}{(\sigma_i^l)^2}(|x_i - x_i^l| - (x_i - x_i^l))^2 + \frac{1}{(\sigma_i^u)^2}(|x_i - x_i^u| + (x_i - x_i^u))^2\right] \quad (4)$$

In the J_{obs} part of cost function (Eq. 3), x is the vector of model parameters (Table 2), $F_i(x)$ is the observation operator that maps parameters x to observation space at the ith time step, y_i is the vector of carbon flux observations at the ith time step. Specifically, y_i is $\begin{bmatrix} \text{GPP}_i \\ \text{NEP}_i \end{bmatrix}$ for site-level parameterization that uses AmeriFlux GPP and NEP; and $y_i = [\text{GPP}_i]$ for spatially explicit

parameterization, which uses MODIS GPP product. N denotes the total number of time steps over assimilation time window. R^{-1} is the inverse of observation error covariance matrix. J_{prior}, part of the cost function (Eq. 4), characterizes the deviation between the updated parameters x_i and our prior knowledge including parameters upper bound x_i^u and lower bound x_i^l (Table 2). J_{prior} provides a feasible way to incorporate the knowledge about parameter empirical upper bound and lower bound into J, and more importantly still preserves the convexity of the cost function J (Schartau et al. 1999). A parameter that falls into the empirical range $[x_i^l \quad x_i^u]$ has no effect on J. Conversely, any parameter that falls out of its empirical range would be panelized by enhancing J_{prior}. σ_i^l and σ_i^u are set to 0.0001% of x_i^l and x_i^u, respectively, in order to ensure the estimated parameters are constrained within their bounds.

Since the cost function is convex, the minimal point could be iteratively found. The adjoint version of TEM supplies the gradient of the cost function with respect to parameters ($\nabla_p J$) in each iteration. The gradient descent algorithm (Natvik et al. 2000) that minimizes the cost function and optimizes model parameters is used (Eq. 5):

$$x_{\text{new}} = x - \alpha \nabla_p J \tag{5}$$

Where x_{new} is the vector of updated parameters in each iteration, x is the vector of parameters in previous iteration. α is the step size. Twenty-six model parameters were calibrated in this study. Table 2 has a detailed description for each model parameter including prior knowledge such as maximum and minimum values (Tang and Zhuang 2009).

Two types of model simulations were conducted with different parameterization methods. For traditional site-level parameterization and extrapolation (hereafter referred to as site-TEM), we used GPP and NEP data to calibrate the model. Specifically, Howland Forest Main site's six years data (1996–2001) were used to calibrate temperate coniferous forest. Six years data (1992–1997) from Harvard Forest site were used to constrain temperate deciduous forest. Vaira Ranch data (2001–2003) were used to calibrate grassland. Lost Creek data (2001–2003) were used for shrub land parameterization and UCI_1850's three-year data (2002–2004) were used for boreal forest calibration. The rest of AmeriFlux data at each site was used to evaluate the performance of the model. The optimal parameters were then extrapolated to the conterminous United States. Each PFT shares the same set of optimal parameters in the region.

The second type of simulations was base on the spatially explicit parameterization method (hereafter referred to as spatial-TEM). We used (2000–2004) monthly MODIS GPP product (Zhao et al. 2005) to parameterize TEM for each 0.5° by 0.5° resolution grid cell. The MODIS GPP product of year 2005 was used for model verification. The spatially explicit parameters were then used to quantify carbon dynamics in the conterminous U.S. from 2000 to 2005.

Model evaluation

We compared the simulations of site-TEM and spatial-TEM with satellite-based GPP of year 2005. We examined the spatial differences and their seasonality of the simulated GPP with two methods for different PFTs. For NEP, there is no regional observational data for direct comparison. We therefore indirectly evaluated the simulations using a coupled top-down and bottom-up approach. Specifically, we fed the estimated NEP into an atmospheric transport model, GEOS-Chem (Suntharalingam et al. 2003, Suntharalingam et al. 2004, Suntharalingam et al. 2005, Nassar et al. 2010) to estimate the temporal evolution and spatial distribution of near surface CO_2 concentrations. We then compared the flask observations and the modeled surface CO_2 concentrations from GEOS-Chem. To evaluate the NEP over the conterminous United States, we also conducted the spatially explicit model parameterization and NEP simulations for other regions beyond the United States. Therefore in GEOS-Chem simulations, only NEP over the conterminous United States was different between site-TEM and spatial-TEM. The GEOS-Chem version 9-01-02 used here aggregates the surface CO_2 signals from the ocean (Takahashi et al. 2009), fossil fuel consumption, cement manufacture (Andres et al. 2011), biomass burning emissions (van der Werf et al. 2006), biofuel combustion emissions (Yevich and Logan 2003), shipping emissions (Corbett and Koehler 2003), aviation emissions

Table 3. Optimal parameters from site-level parameterization.

ID	Abbreviation	Boreal	Coniferous	Deciduous	Grassland	Shrub land
1	C_{max}	961.92	1072.05	1141.02	778.11	521.03
2	K_I	66.11	44.03	97.61	212.91	73.95
3	K_C	203.42	185.54	219.83	244.09	271.36
4	T_{max}	29.48	33.94	30.60	33.74	41.08
5	T_{min}	−8.38	−4.26	0	0	−0.32
6	T_{opt}	22.4	30	30.9	32.7	35.10
7	ALEAF	0.54	0.65	0.59	0.37	0.53
8	BLEAF	0.51	0.55	0.68	0.39	0.66
9	CLEAF	0.31	0.38	0.18	0.20	0.052
10	MINLEAF	0.47	0.490	0.02	0.14	0.276
11	N_{max}	52.84	21.77	49.15	22.74	94.0
12	K_{n1}	0.0042	0.0042	0.17153	0.0042	0.0042
13	RAQ10A0	2.43	2.34	2.26	2.31	2.56
14	RAQ10A1	−0.0531	−0.052	−0.023	−0.053	−0.053
15	RAQ10A2	0.0023	0.0023	0.0024	0.0023	0.0023
16	RAQ10A3	-4.1×10^{-5}	-4.1×10^{-5}	-6×10^{-5}	-4.1×10^{-5}	-4.1×10^{-5}
17	KDC	0.0027	0.0038	0.0046	0.0051	0.0048
18	RHQ10	1.81	1.84	1.99	2.42	2.19
19	MOISTMAX	0.98	0.90	0.93	0.98	1
20	MOISTMIN	0	0	0	0	0
21	MOISTOPT	0.54	0.45	0.46	0.39	0.49
22	N_{up}	24.36	6.73	7.03	17.22	59.42
23	K_{n2}	0.0042	0.218	0.25	0.0042	0.0042
24	CFALL	0.0017	0.00469	0.0050	0.052	0.013
25	NFALL	0.0089	0.01043	0.015	0.031	0.0089
26	KRC	0.0029	0.0032	0.0020	0.016	0.014

(Friedl 1997), chemical source (Nassar et al. 2010), and net ecosystem exchanges. The atmospheric transportation (Staniforth and Cote 1991, Zhang and McFarlane 1995) modeled a three-dimensional distribution of atmospheric CO_2. Its spatial resolution is 4° by 5° (latitude by longitude) and its temporal resolution is 15 minutes for atmospheric transport and convection, and 60 minutes for emissions.

We detrended the modeled CO_2 concentration time series and obtained the seasonal component by using a seasonal-trend decomposition procedure LOESS (Cleveland et al. 1990). Then the modeled seasonal variation of the surface CO_2 concentrations was compared with the observational surface CO_2 at six U.S. monitoring stations of the GLOBALVIEW-CO2 observation network including CMO at Oregon, HDPDTA at Utah, KEY at Florida, MLO at Hawaii, NWR at Colorado, and OPW at Washington (Herbert et al. 1986, Komhyr et al. 1989, Thoning 1989, Bakwin et al. 1995, Masarie and Tans 1995, Masarie et al. 2001, GLOBALVIEW-CO2 2012). A better match between the observed and simulated CO_2 concentrations at these stations will indicate better NEP estimates.

Results and Discussion

Optimal parameters calibrated with the adjoint method

The conterminous U.S. is covered by five major plant functional types (PFT) including temperate coniferous forest, temperate deciduous forest, grassland, shrub land and boreal forest. Thus, we parameterized site-TEM for these five PFTs (Table 3). For the spatial-TEM, we parameterized the model for each grid cell in the region using satellite-based GPP data. The optimal parameters for each PFT with their means and standard deviations were documented in Table 4. Some parameters were unable to be calibrated for spatial-TEM, because the MODIS GPP product is insensitive to those parameters. For example, Q10 for heterotrophic respiration (RHQ10) and other three parameters related to soil moisture effects on heterotrophic respiration (MOISTMAX, MOISTMIN, MOISTOPT) were not optimized (Table 4). The MODIS GPP product measures the aboveground carbon production through plant photosynthesis, thus has no constraints on heterotrophic respiration occurred in soils.

The spatial distribution of the optimal parameters reveals the spatial heterogeneity of ecosys-

Table 4. Optimal parameters from spatially explicit parameterization.

ID	Abbreviation	Boreal	Coniferous	Deciduous	Grassland	Shrub land
1	C_{max}	742.5 ± 57.6	858.5 ± 77.6	1131.8 ± 65.5	725.4 ± 90.3	602.8 ± 167.9
2	K_I	101.5 ± 25.5	61.8 ± 20.1	100.6 ± 16.9	122.8 ± 26.6	74.9 ± 20.4
3	K_C	349.9 ± 46.5	261.9 ± 38.3	312.2 ± 50.2	247.4 ± 42.8	272.3 ± 67.9
4	T_{max}	28.22 ± 0.70	32.71 ± 1.05	30.37 ± 1.30	36.67 ± 1.06	42.84 ± 1.71
5	T_{min}	−6.23 ± 0.78	−2.32 ± 0.92	0 ± 0	0 ± 0	−0.67 ± 0.96
6	T_{opt}	22.38 ± 0.11	29.99 ± 0.066	30.90 ± 0.001	32.69 ± 0.001	35.09 ± 0.001
7	ALEAF	0.42 ± 0.056	0.49 ± 0.059	0.73 ± 0.066	0.49 ± 0.082	0.53 ± 0.055
8	BLEAF	0.31 ± 0.051	0.39 ± 0.050	0.39 ± 0.77	0.53 ± 0.069	0.71 ± 0.057
9	CLEAF	0.26 ± 0.030	0.30 ± 0.027	0.52 ± 0.050	0.31 ± 0.035	0.13 ± 0.064
10	MINLEAF	0.48 ± 0.022	0.51 ± 0.023	0.02 ± 0.012	0.1 ± 0.009	0.26 ± 0.028
11	N_{max}	52.6 ± 2.2	21.4 ± 0.2	49.3 ± 0.6	22.8 ± 0.4	74.9 ± 4.4
12	K_{n1}	0.006 ± 0.002	0.004 ± 0.001	0.004 ± 0.001	0.004 ± 0.003	0.005 ± 0.001
13	RAQ10A0	2.34 ± 0.043	2.29 ± 0.17	2.76 ± 0.11	2.49 ± 0.18	2.50 ± 0.35
14	RAQ10A1	$-0.053 \pm 3 \times 10^{-5}$	−0.052 ± 0.0003	−0.0030 ± 0.0018	−0.052 ± 0.00035	−0.052 ± 0.0002
15	RAQ10A2	$0.002 \pm 2 \times 10^{-7}$	$0.002 \pm 1 \times 10^{-5}$	$0.003 \pm 1 \times 10^{-6}$	$0.002 \pm 1 \times 10^{-7}$	$0.002 \pm 1 \times 10^{-6}$
16	RAQ10A3	$-4 \times 10^{-5} \pm 0$	$-4 \times 10^{-5} \pm 1 \times 10^{-7}$	$-7 \times 10^{-5} \pm 1 \times 10^{-6}$	$4 \times 10^{-5} \pm 2 \times 10^{-7}$	$4 \times 10^{-5} \pm 1 \times 10^{-7}$
17	KDC	0.001 ± 0	0.003 ± 0.0005	0.004 ± 0.0003	0.003 ± 0.0006	$0.003 \pm 5 \times 10^{-5}$
18	RHQ10	2	2	2	2	2
19	MOISTMAX	1	1	1	1	1
20	MOISTMIN	0	0	0	0	0
21	MOISTOPT	0.5	0.5	0.5	0.5	0.5
22	N_{up}	24.36 ± 0.001	7.11 ± 0.46	6.06 ± 0.19	17.5 ± 1.68	30.15 ± 4.83
23	K_{n2}	0.004 ± 0	0.01 ± 0.005	0.008 ± 0.003	0.01 ± 0.006	0.05 ± 0.01
24	CFALL	$0.002 \pm 6 \times 10^{-5}$	0.004 ± 0.0008	0.003 ± 0.0004	0.04 ± 0.004	0.01 ± 0.002
25	NFALL	$0.007 \pm 1 \times 10^{-5}$	0.01 ± 0.008	0.02 ± 0.002	0.02 ± 0.003	0.009 ± 0.001
26	KRC	0.006 ± 0	0.001 ± 0.0004	0.003 ± 0.0005	0.01 ± 0.0008	0.006 ± 0.0001

tem and biogeochemical processes. Since the maximum rate of photosynthesis C (C_{max}), plant respiration rate at 0°C (KRC), heterotrophic respiration rate at 0°C (KDC), proportion of vegetation carbon loss as litterfall monthly (CFALL), ratio between N immobilized and C respired (N_{up}) and maximum rate of N uptake by vegetation (N_{max}) were identified as controlling parameters in modeling carbon fluxes (Chen and Zhuang 2012), we thus focused our analysis on the six parameters. These six parameters had a large spatial variability (Fig. 1). High values of C_{max} resided in the regions around Ozark plateaus, the Ouachita Mountains and also along the eastern and western coastlines. Low values of C_{max} existed in the area of Oregon, Idaho and western part of Texas. The values of KRC were relatively high in the central U.S. and low in the eastern and western U.S. Highest KDC appeared in some small regions in the states of Wyoming, Colorado and New Mexico and also in southern edge of Florida. Lowest KDC appeared in eastern Utah and northeastern Minnesota. The spatial distributions of CFALL and N_{up} were similar to some extent. High parameter values appeared in the interior of U.S., while lower parameter values were in the eastern part of U.S. and western coastal area. However, they were different in spatial variations in the interior of U.S. CFALL values varied in Mountain area of eastern U.S., while N_{up} significantly varied in central U.S. High N_{max} values were clustered in the northeastern Minnesota and also in some small regions of eastern U.S. Mountain area, while low values were located in large areas of central U.S. and the coastal regions. Chen and Zhuang (2012) (hereafter referred to as Chen2012) conducted a similar study for U.S. forest ecosystems only. There are similarities and differences between the optimal model parameters in Chen2012 and our estimations for U.S. forest ecosystems. For example, both showed the high values of C_{max} in Ozark plateaus, the Ouachita Mountains areas. Chen2012 claimed that high C_{max} values were also in the coastal regions of Washington and Oregon, but relatively low in our estimates. The two studies agreed that low KRC values were located in Washington and Oregon. Chen2012 showed that, in the U.S. South Atlantic regions, KRC was higher than that in the U.S. East North Central regions, while our results showed an opposite comparison. Chen2012 concluded that high KDC values were mostly distributed in the Appalachian Mountains area; however our esti-

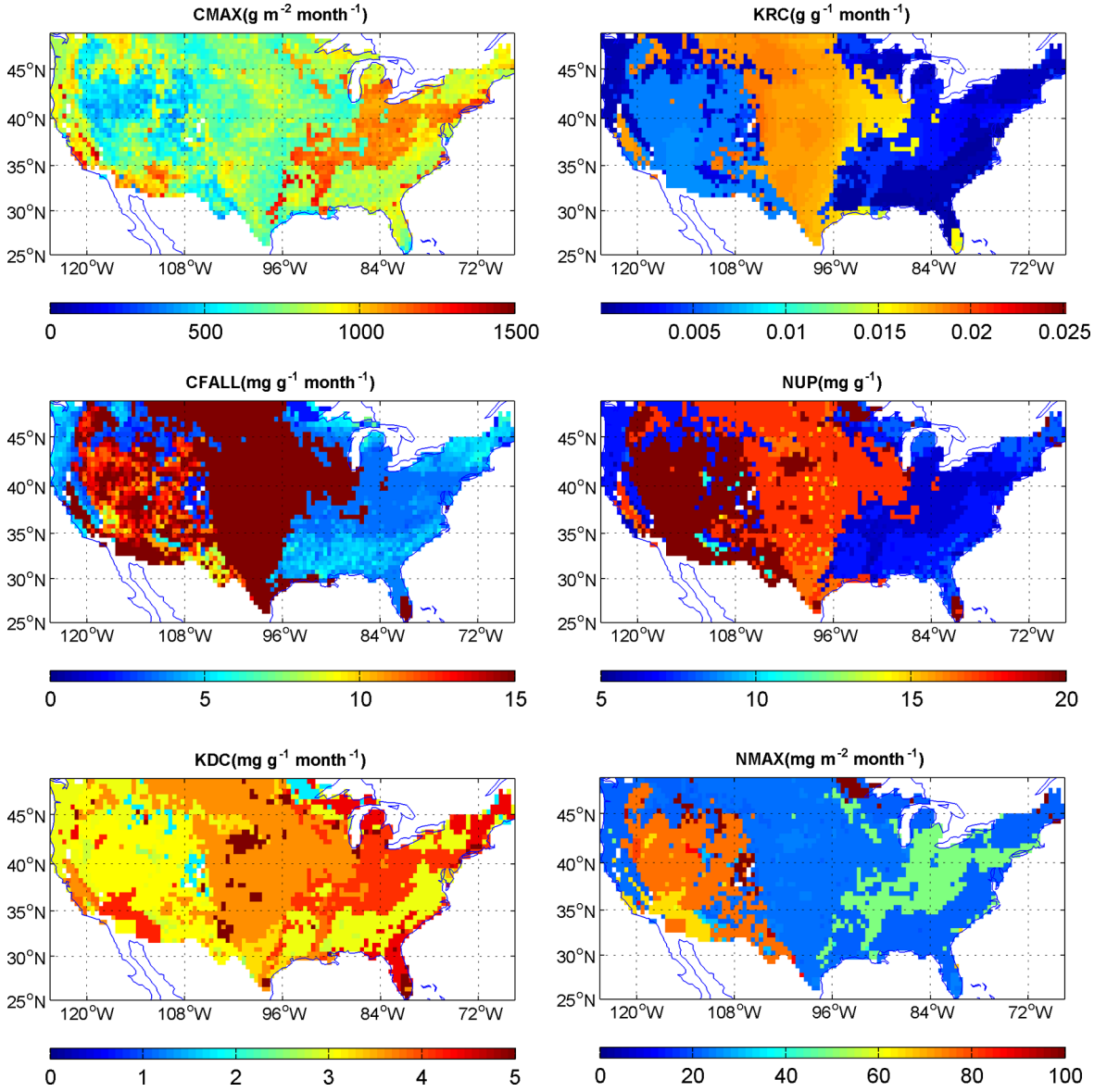

Fig. 1. Spatial distributions of six key parameters in TEM.

mates are in New England region and state of Florida. For CFALL, the areas along the Gulf Coast are high in Chen2012 and low in our estimates. The N_{up} and N_{max} had similar spatial patterns in Chen2012. They concluded that parameters values were high in the southern coastal plains, the northern central areas and low in the east-central United States. We found that N_{max} was low in the southern coastal plains instead. A number of reasons caused these differences. For example, Chen2012 used annual GPP observations while our study used monthly GPP, which constrain parameters differently. The primary DA goal of Chen2012 was to capture annual GPP rather than monthly GPP. In addition, Chen2012 used a Bayesian approach (Tang and Zhuang 2008, Tang and Zhuang 2009), while we used an adjoint approach. Different computational complexities of these two methods might also contribute to the differences.

The spatial pattern of spatial-TEM parameters' values generally followed the distribution of

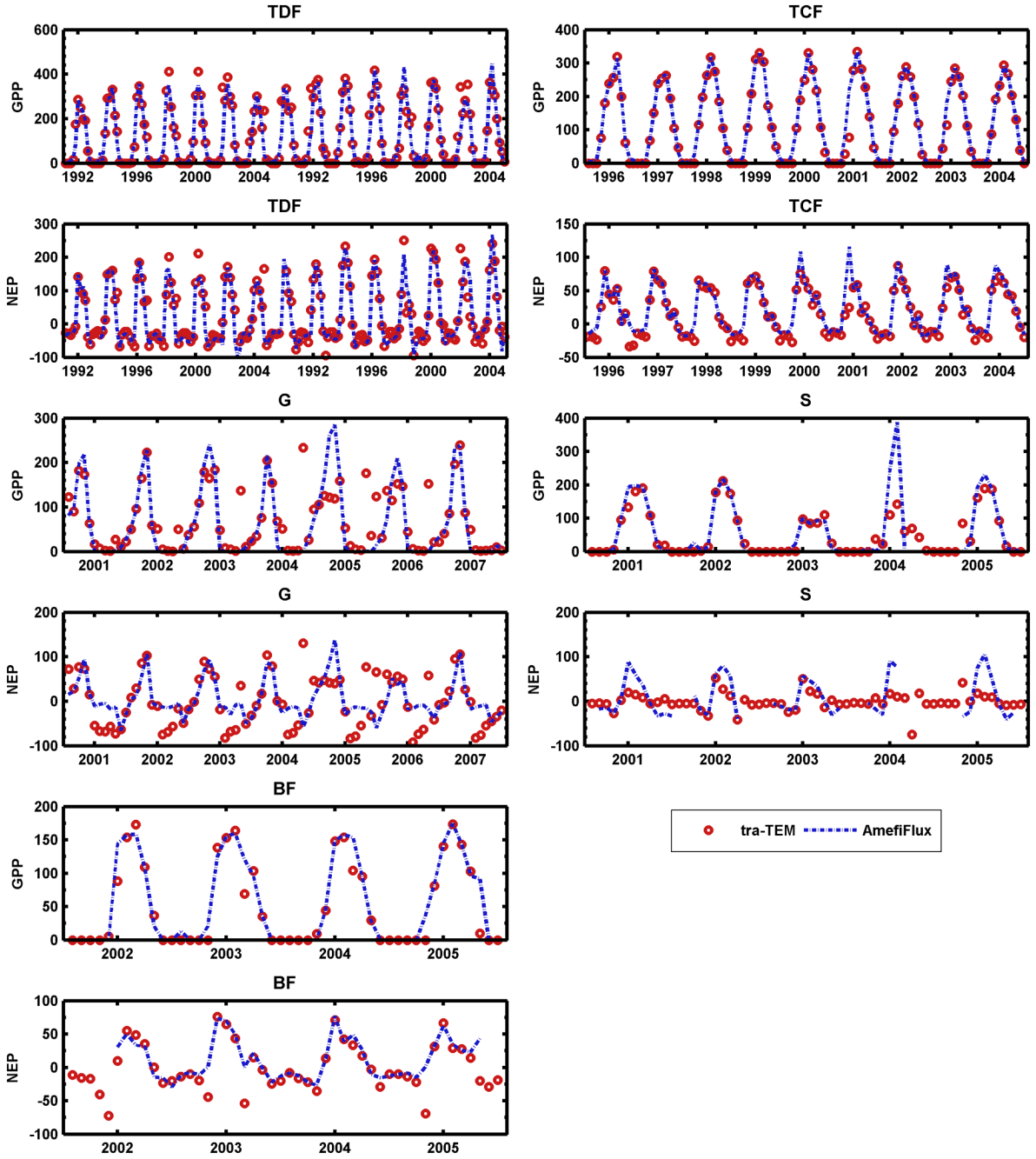

Fig. 2. Site-level simulations conducted for five plant functional types. The trajectories of the modeled GPP and NEP (red circle; g C m^{-2} $month^{-1}$) using the optimal parameters are compared with the AmeriFlux observed GPP and NEP (blue line). (BF: Boreal forest; TCF: Temperate coniferous forest; TDF: Temperate deciduous forest; G: Grassland; S: Shrub land.)

PFTs. It means that model parameters for each PFT may have independent empirical ranges. The empirical ranges mirror the biogeochemical limits of ecosystem processes (e.g., photosynthesis) for different PFTs. While for the same PFT, the model parameters significantly varied with locations. Such heterogeneity of ecosystem is due to several causes including variation of vegeta-

Table 5. Model-data fitting statistics: the carbon dynamics of GPP and NEP modeled using the site-level parameterization method are compared with the AmeriFlux observations.

Simulated carbon fluxes	R^2	Slope	Intercept
Boreal forest			
GPP	0.92	0.93	−1.37
NEP	0.73	1.00	−7.64
Temperate coniferous forest			
GPP	0.98	1.01	−5.98
NEP	0.89	0.92	−3.24
Temperate deciduous forest			
GPP	0.89	0.98	10.45
NEP	0.85	0.91	8.89
Grassland			
GPP	0.60	0.65	30.60
NEP	0.41	0.89	−5.38
Shrub land			
GPP	0.78	0.67	14.52
NEP	0.41	0.29	−0.49

tion structure (Bondeau et al. 1999), plant species (Cardinale et al. 2000), forest stand age (Gower et al. 1996, Pregitzer and Euskirchen 2004, Zaehle et al. 2006, He et al. 2012), species differences in leaf longevity (Kitajima et al. 1997), and local agriculture management (Rounsevell et al. 2003). Satellite-based MODIS GPP is a function of all these factors, thus well represents the spatial heterogeneity of aboveground ecosystem structure and functioning. By assimilating MODIS GPP into TEM, the parameters associated with aboveground ecosystem processes were well constrained for each grid cell in the region.

Model evaluation

Site-TEM modeled GPP and NEP are compared well with the AmeriFlux observations (Fig. 2). Model-data fitting statistics including the Pearson correlation coefficients (R^2) and first order linear regression slope and intercept showed that site-TEM generally worked better in boreal, coniferous and deciduous forests than in grassland and shrub land (Table 5). When extrapolating the grassland and shrub land site-level optimal parameters to the region, the uncertainty was amplified. Similarly, the regional simulations for forest ecosystems were also of a large uncertainty. These uncertainties were due to the fact that the site-level parameterization is assumed with no- change for the same PFT over the region.

Spatially explicit parameters helped reduce model simulation uncertainties because they were calibrated for each grid cell. Regional distributions of annual GPP from both spatial-TEM and site-TEM simulations were compared with the MODIS GPP (Fig. 3). The spatial-TEM estimated the regional annually-aggregated GPP was 6.87 Pg C yr^{-1} (1 Pg $= 10^{15}$ g) in 2005. There was 0.28 Pg C yr^{-1} or 4% biases in comparison with the MODIS observation of 6.59 Pg C yr^{-1}. Moreover, spatial-TEM generally agreed with the MODIS data in terms of spatial distribution, except for a slight overestimation in the mid-east area. The site-TEM annual GPP was 5.95 Pg C yr^{-1} in 2005, which was 0.64 Pg C yr^{-1} or 10% lower than the observations. The spatial distribution greatly differed from observations. The greatest discrepancies existed in the western (Washington, Oregon, California) and southeastern (Georgia, Alabama, Florida) coastal areas and in the northeastern central area (Illinois, Indiana, Ohio). In comparison, the spatially explicit parameterization method tends to more adequately account for the spatial heterogeneity of ecosystems in the regional simulations.

To reveal the magnitude of spatial ecosystem heterogeneity, we partitioned the regional GPP according to PFTs. We found that grassland, temperate deciduous forest and boreal forest had the greatest spatial heterogeneity (Fig. 4). In grassland, the site-TEM greatly underestimated GPP. In temperate deciduous forest and boreal forests, the site-TEM overestimated GPP. Such regional model-data misfits were due to the site-level calibration and extrapolation. For example, site-TEM grassland was parameterized at Vaira Ranch site. Because the Vaira Ranch site in California is affected by the Mediterranean climate, which is dry and hot in summer. Precipitation occurs from October to May and the growing season typically ends in May. After May, the grass gradually dies due to high temperature and dry environmental conditions. The seasonality of GPP was well captured by site-TEM (Fig. 5). However, the parameters obtained at the Vaira Ranch site does not work for other grasslands grid cells in the region.

Spatially, the overestimation in grasslands compensated the underestimation in boreal forests and temperate deciduous forests, resulting in the regional GPP from site-TEM did not differ much from the observations. The regional

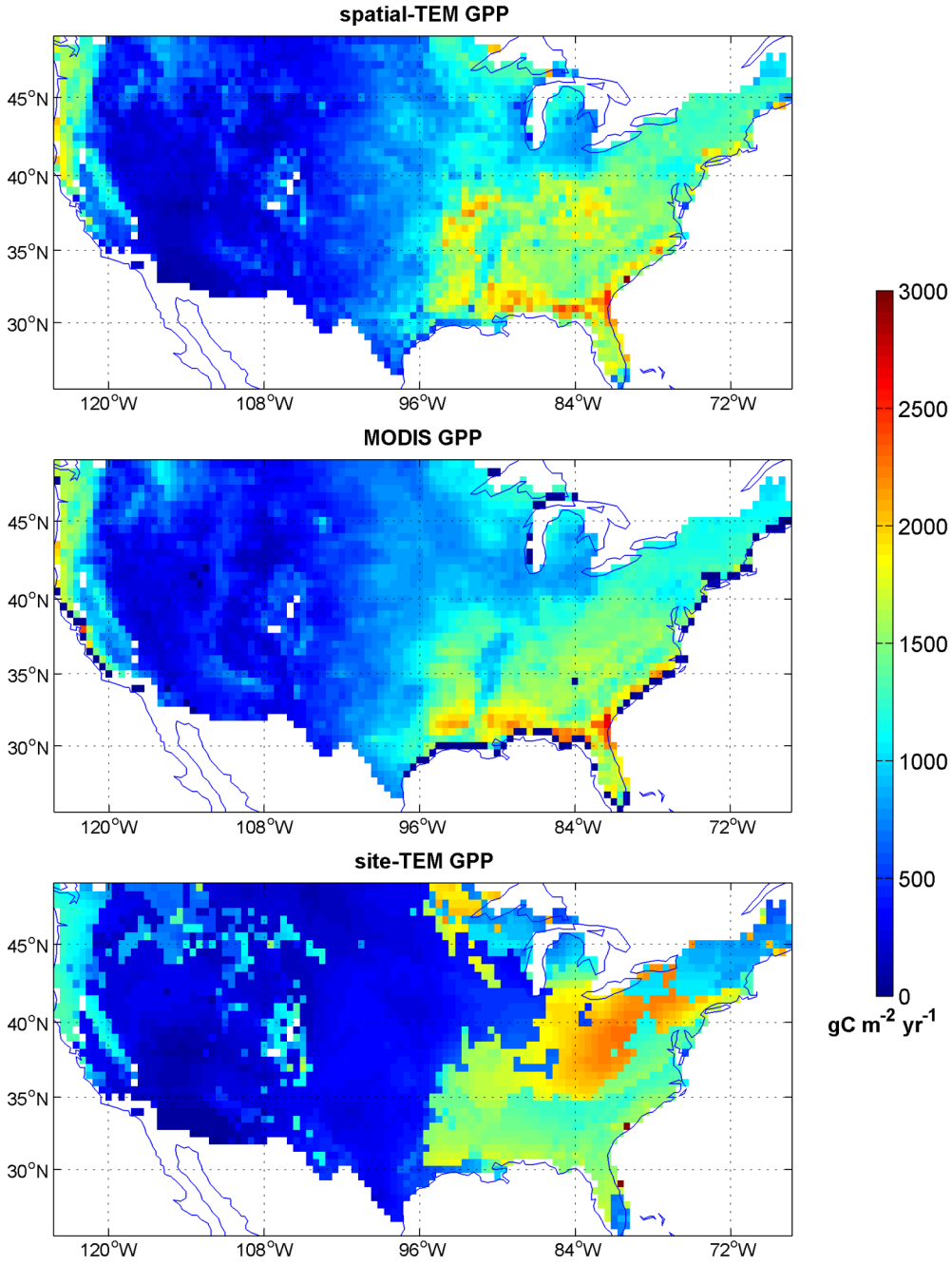

Fig. 3. Annual GPP (g C m^{-2} $year^{-1}$) over the conterminous United States in 2005. The upper panel is the TEM-modeled GPP by applying the spatially explicit parameters. The middle panel is MODIS GPP in 2005 and the lower panel is TEM-modeled GPP with site-level parameterization method using AmeriFlux data.

GPP seasonal cycle simulated with the site-TEM also fitted observations well (Fig. 5).

The spatial-TEM estimated NEP was 0.74 Pg C yr^{-1} for the conterminous U.S. in 2005, while the site-TEM only estimated 0.21 Pg C yr^{-1}. Since there is no regional observational NEP for direct comparison, we used an atmospheric transport model (GEOS-Chem) to indirectly evaluate the

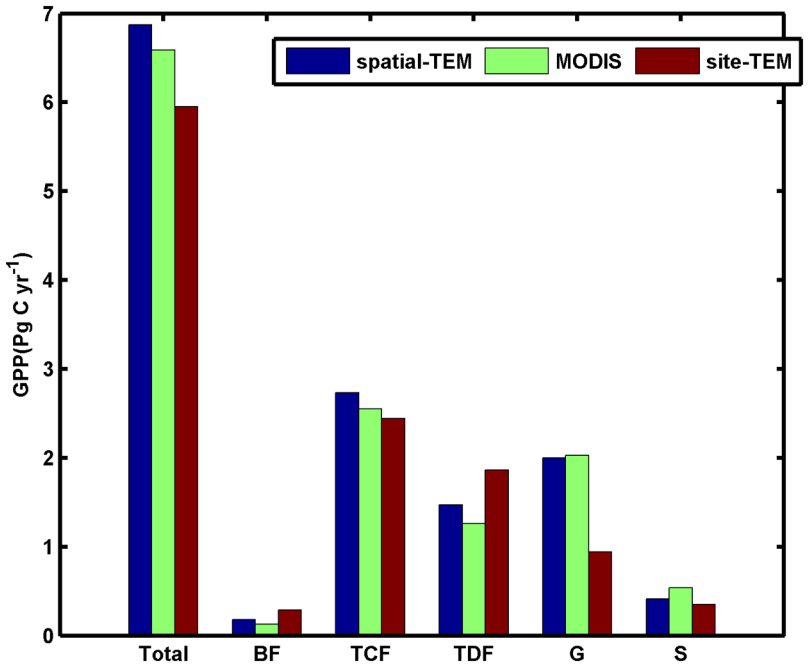

Fig. 4. Regional GPP (Pg C year^{-1}; 1 Pg = 10^{15} g) in 2005. The largest differences between spatial-TEM and site-TEM exist in grasslands. (BF: Boreal forest; TCF: Temperate coniferous forest; TDF: Temperate deciduous forest; G: Grassland; S: Shrub land.)

NEP simulated with site-TEM and spatial-TEM. The surface net carbon exchanges between terrestrial ecosystems and the atmosphere were different between two TEM simulations, affecting the seasonality of atmospheric CO_2 concentrations (Fig. 6). The root mean squared errors (RMSE) between the spatial-TEM and observations were 1.7, 1.9, 1.15, 0.5, 1.6, 0.5, 1.6, and 1.3 (ppm) at CMO, HDPDTA, KEY, MLO, NWR, OPW, respectively. In contrast, the RMSE between the site-TEM simulation and observations were much larger: 4.0, 2.9, 1.9, 1.2, 2.7, 3.9 (ppm) at six monitoring stations, respectively. These results suggested that spatial-TEM better estimated regional NEP.

Conclusions

We used a process-based biogeochemistry model, the Terrestrial Ecosystem Model, to simulate the carbon dynamics over the conterminous United States with two model parameterization methods. One method parameterized TEM at site-level with AmeriFlux data (site-TEM) and then extrapolated the optimal parameters to the region. The second method was a spatially explicit parameterization approach using satellite-based MODIS GPP (spatial-TEM). We concluded that the spatial pattern of the optimized parameters generally follows the PFT distribution. More importantly, the parameter values for each PFT also significantly vary across the space. This finding is consistent with several other spatially explicit data assimilation studies (e.g., Zhou et al. 2009, Zhou et al. 2012). We also concluded that the spatial-TEM better captured spatial distribution, seasonal and annual carbon dynamics. The conterminous U.S. annual GPP was 6.87 Pg C yr^{-1} simulated with spatial-TEM and 5.95 Pg C yr^{-1} with the site-TEM, while satellite-based estimation was 6.59 Pg C yr^{-1}. The spatial distribution pattern of GPP from spatial-TEM agreed well with observations. The spatial-TEM estimated NEP of 0.74 Pg C yr^{-1} for the conterminous U.S. in 2005, while the site-TEM only estimated 0.21 Pg C yr^{-1}, which was 72% smaller. The modeled NEP from the two methods was evaluated by conducting two sets of GEOS-Chem simulations and comparing the simulated near surface atmospheric CO_2 concentrations with the flask measurements. Driven with

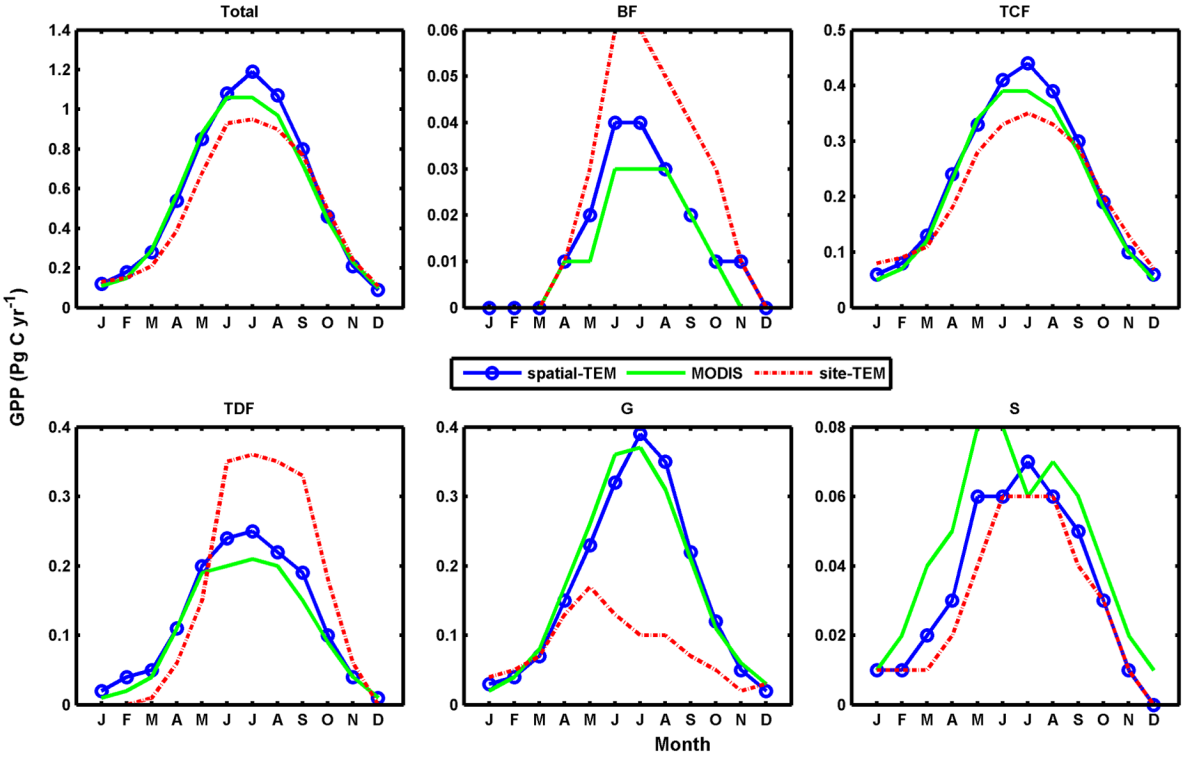

Fig. 5. Seasonal variability of regional GPP (Pg C year^{-1}; 1 Pg = 10^{15} g) for each PFT. The variability shows that site-TEM significantly overestimates the GPP seasonal changes in boreal forests and temperate deciduous forests, while it underestimates the GPP seasonality in grasslands. (BF: Boreal forest; TCF: Temperate coniferous forest; TDF: Temperate deciduous forest; G: Grassland; S: Shrub land.)

spatial-TEM estimated NEP, GEOS-Chem better captured the seasonal variation of surface CO_2. Our study suggested that the future quantification of terrestrial ecosystem dynamics should use the available spatial information to parameterize the ecosystem models in a spatially explicit manner so as to account for the effects of spatial heterogeneity of regional ecosystems on carbon cycling. In addition, our study indicated that the adjoint approach was an effective approach to assimilate both in situ and satellite-based data to improve ecosystem model parameterization.

This study has several limitations. First, MODIS GPP data are model results using the MOD17 algorithms, which are calibrated for representative PFTs. Thus GPP data is not strictly spatially explicit. However, since fPAR is the most important variable in the MOD17 algorithms, and is spatially explicit, we thus treated the MODIS GPP as spatially explicit. Our study demonstrated the satellite-based GPP information indeed helped improve regional simulations. Second, our results showed that parameters associated with soil processes were not well calibrated using MODIS GPP. This is mainly due to the fact that MODIS GPP data is lack of information to constrain the parameters associated with soil processes including Q10 for heterotrophic respiration (RHQ10) and other three parameters related to soil moisture effects on heterotrophic respiration (MOISTMAX, MOISTMIN and MOISTOPT)). It has been pointed out that a specific dataset is only able to constrain a subset of model parameters in other studies. For example, Barrett (2002) found that NPP data could only directly constrain some parameters associated with leaf processes (i.e., maximum light-use efficiency, allocation of NPP to leaves, carbon residence time of leaf). Xu et al. (2006) found that even using data of one carbon flux (soil respiration) and five pools (woody biomass, foliage biomass, litter fall, C in litter layers and C in mineral soil), some parameters

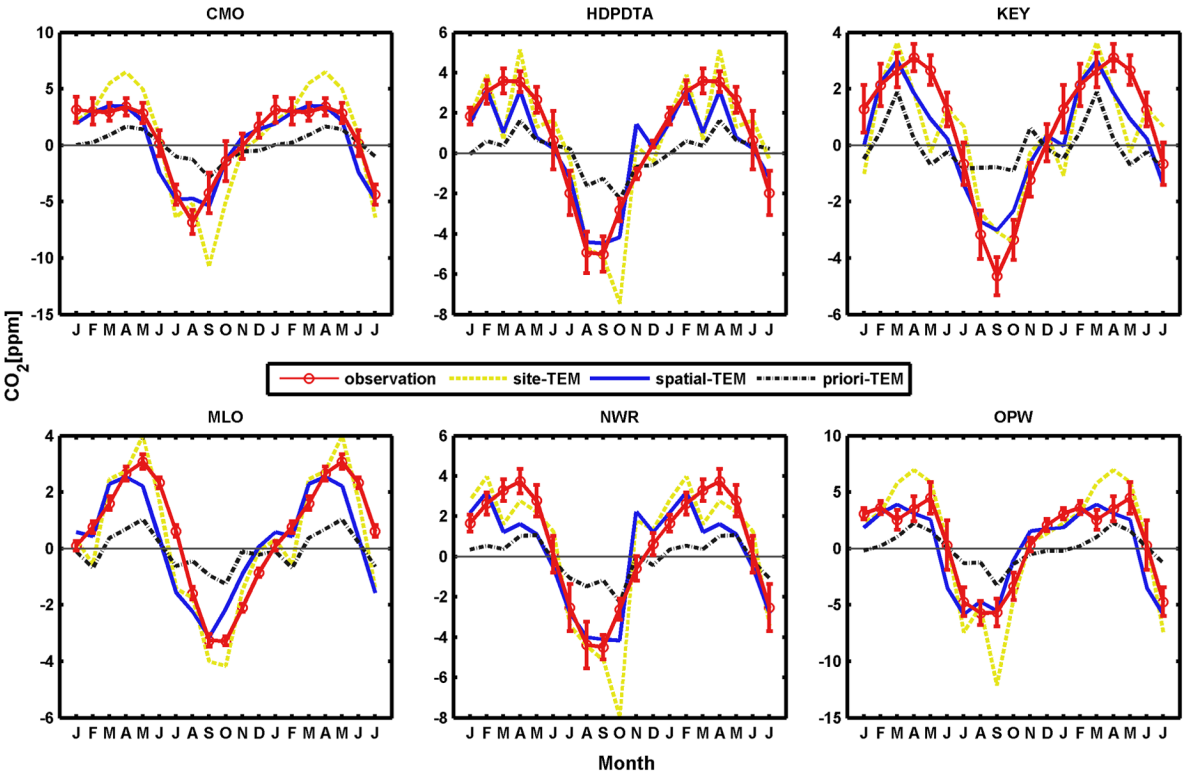

Fig. 6. Seasonal trends of surface CO_2 concentrations (ppm) at six GLOBALVIEW-CO2 observation stations. The GEOS-Chem CO_2 simulation results driven by NEP estimated with spatial-TEM (blue solid), site-TEM (yellow dash) and priori-TEM (grey dash) are compared with observations (red solid line with error bar). The error bars show the standard deviations for the observation data.

associated with underground processes (i.e., transfer coefficients from pools of metabolic litter, microbe and passive soil C) were still not well constrained. Previous data assimilation studies have noticed that combining multiple sources of information including ecosystem fluxes and pools data could in general help reduce parameter uncertainty (e.g., Barrett 2002, Xu et al. 2006, Zhou and Luo 2008, Zhou et al. 2012). We thus speculate that the spatial-TEM could be improved by utilizing other spatially explicit soil carbon pool data in addition to MODIS GPP. For instance, Zhou et al. (2009) showed that soil carbon content data is tightly related to soil respiration Q10, therefore could be used to calibrate Q10 in CASA model (the same parameter as TEM's RHQ10). Therefore, soil property data such as Harmonized World Soil Database (FAO/IIASA/ISRIC/ISS-CAS/JRC 2012) or Soil Organic Carbon database (Global Soil Data Task 2000) may be useful in our spatially explicit calibration of RHQ10, MOISTMAX, MOISTMIN, MOISTOPT in future study. Third, we obtained optimal parameters using the adjoint method. However the uncertainties of these parameters were not quantified. Previous studies indicated that, at the minimal point of the cost function, the inverse of Hessian can describe the uncertainty of optimal parameters (Tarantola 1987, Rayner et al. 2005, Scholze et al. 2007). Such conclusion is valid as long as the distribution of model parameters is multivariate normal. In our study, model parameters were assumed to uniformly distribute between their empirical upper and lower bounds (Table 2). Thus, instead using the inverse-of-Hessian method, new methods are needed to quantify the uncertainty of our model parameters.

Acknowledgments

We thank two anonymous reviewers to help

improve our earlier version of the manuscript. We acknowledge the eddy flux network principal investigators for providing carbon flux data. This research is supported by NASA Land Use and Land Cover Change program (NASA- NNX09AI26G), Department of Energy (DE-FG02-08ER64599), National Science Foundation (NSF-1028291 and NSF- 0919331), the NSF Carbon and Water in the Earth Program (NSF-0630319), and a NSF CDI Type II project (IIS- 1028291).

Literature Cited

Alton, P., L. Mercado, and P. North. 2007. A sensitivity analysis of the land-surface scheme JULES conducted for three forest biomes: Biophysical parameters, model processes, and meteorological driving data. Global Biogeochemical Cycles. doi: 10.1029/2005GB002653

Andres, R. J., J. S. Gregg, L. Losey, G. Marland, and T. A. Boden. 2011. Monthly, global emissions of carbon dioxide from fossil fuel consumption. Tellus B 66:309–327.

Bakwin, P. S., P. P. Tans, C. Zhao, W. Ussler, III, and E. Quesnell. 1995. Measurements of carbon dioxide on a very tall tower. Tellus B 47:535–549.

Baldocchi, D. D., et al. 2005. Predicting the onset of net carbon uptake by deciduous forests with soil temperature and climate data: a synthesis of FLUXNET data. International Journal of Biometeorology 49:377–387.

Baldocchi, D. D., L. Xu, and N. Kiang. 2004. How plant functional-type, weather, seasonal drought, and soil physical properties alter water and energy fluxes of an oak-grass savanna and an annual grassland. Agricultural and Forest Meteorology 123:13–39.

Baldocchi, D. D. 2003. Assessing the eddy covariance technique for evaluating carbon dioxide exchange rates of ecosystems: past, present and future. Global Change Biology 9:479–492.

Baldocchi, D. D., et al. 2001. FLUXNET: a new tool to study the temporal and spatial variability of ecosystem-scale carbon dioxide, water vapor and energy flux densities. Bulletin of the American Meteorological Society 82:2415–2435.

Barrett, D. J. 2002. Steady state turnover time of carbon in the Australian terrestrial biosphere. Global Biogeochemical Cycles 16:1–21.

Bondeau, A., D. W. Kicklighter, J. Kaduk, and the participants of the Potsdam NPP Model Intercomparison. 1999. Comparing global models of terrestrial net primary productivity (NPP): Importance of vegetation structure on seasonal NPP estimates. Global Change Biology 5:35–45.

Bond-Lamberty, B., C. Wang, and S. T. Gower. 2005. Spatiotemporal measurement and modeling of stand-level boreal forest soil temperatures. Agricultural and Forest Meteorology 131:27–40.

Braswell, B. H., W. J. Sacks, E. Linder, and D. S. Schimel. 2005. Estimating diurnal to annual ecosystem parameters by synthesis of a carbon flux model with eddy covariance net ecosystem exchange observations. Global Change Biology 11:335–355.

Cacuci, D. G. 1981*a*. Sensitivity theory for nonlinear systems. I. Nonlinear functional analysis approach. Journal of Mathematical Physics 22:2794–2802.

Cacuci, D. G. 1981*b*. Sensitivity theory for nonlinear systems. II. Extensions to additional classes of responses. Journal of Mathematical Physics 22:2803–2812.

Cardinale, B. J., K. Nelson, and M. A. Palmer. 2000. Linking species diversity to the functioning of ecosystems: on the importance of environmental context. Oikos 91:175–183.

Carmillet, V., J. M. Brankart, P. Brasseur, H. Drange, G. Evensen, and J. Verron. 2001. A singular evolutive extended Kalman filter to assimilate ocean color data in a coupled physical-biochemical model of the North Atlantic Ocean. Ocean Modelling 3:167–192.

Chen, M., and Q. Zhuang. 2012. Spatially explicit parameterization of a Terrestrial Ecosystem Model and its application to the quantification of carbon dynamics of forest ecosystems in conterminous United States. Earth Interactions 16:1–22.

Cleveland, R. B., W. S. Cleveland, J. E. McRae, and I. Terpenning. 1990. STL: A seasonal-trend decomposition procedure based on loess. Journal of Official Statistics 6:3–73.

Conway, T. J., P. P. Tans, L. S. Waterman, K. W. Thoning, D. R. Kitzis, K. A. Masarie, and N. Zhang. 1994. Evidence for interannual variability of the carbon cycle from the National Oceanic and Atmospheric Administration/Climate Monitoring and Diagnostics Laboratory Global Air Sampling Network. Journal of Geophysical Research: Atmospheres 99:22831–22855.

Corbett, J. J., and H. W. Koehler. 2003. Updated emissions from ocean shipping. Journal of Geophysical Research: Atmospheres. doi: 10.1029/2002JD002898

Evensen, G. 1994. Sequential data assimilation with a nonlinear quasi-geostrophic model using Monte Carlo methods to forecast error statistics. Journal of Geophysical Research: Oceans 99:10143–10162.

FAO/IIASA/ISRIC/ISS-CAS/JRC. 2012. Harmonized World Soil Database. Version 1.2. FAO, Rome, Italy and IIASA, Laxenburg, Austria. http://webarchive.iiasa.ac.at/Research/LUC/External-World-soil-database/HTML

Filed, C. B., J. T. Randerson, and C. M. Malmstrom. 1995. Global net primary production: combining ecology and remote sensing. Remote Sensing of

Environment 51:74–88.

Forster, P., et al. 2007. Changes in Atmospheric Constituents and in Radiative Forcing. Pages 129–234 *in* Solomon, S., D. Qin, M. Manning, Z. Chen, M. Marquis, K.B. Averyt, M.Tignor. and H. L. Miller, editors. Climate change 2007: the physical science basis. Contribution of Working Group I to the Fourth Assessment Report of the Intergovernmental Panel on Climate Change. Cambridge University Press, Cambridge, UK.

Friedl, R. 1997. Atmospheric effects of subsonic aircraft: Interim assessment report of the advanced subsonic technology program. National Aeronautics and Space Administration, Goddard Space Flight Center, Greenbelt, Maryland, USA.

Gao, C., H. Wang, E. Weng, S. Lakshmivarahan, Y. Zhang, and Y. Luo. 2011. Assimilation of multiple data sets with the ensemble Kalman filter to improve forecasts of forest carbon dynamics. Ecological Applications 21:1461–1473.

Giering, R., and T. Kaminski. 1998. Recipes for adjoint code construction. ACM Transactions on Mathematical Software 24:437–474.

Global Soil Data Task. 2000. Global Soil Data Products CD-ROM (IGBP-DIS). International Geosphere-Biosphere Programme, Data and Information System, Potsdam, Germany. http://www.daac.ornl.gov

GLOBALVIEW-CO2. 2012. Cooperative Atmospheric Data Integration Project: carbon dioxide. NOAA ESRL, Boulder, Colorado, USA. http://www.esrl.noaa.gov/gmd/ccgg/globalview

Goulden, M. L., A. M. S. McMillan, G. C. Winston, A. V. Rocha, K. L. Manies, J. W. Harden, and B. P. Bond-Lamberty. 2011. Patterns of NPP, GPP, respiration, and NEP during boreal forest succession. Global Change Biology 17:855–871.

Gower, S. T., R. E. McMurtrie, and D. Murty. 1996. Aboveground net primary production decline with stand age: potential causes. Trends in Ecology & Evolution 11:378–382.

Gurney, K. R., et al. 2002. Towards robust regional estimates of CO_2 sources and sinks using atmospheric transport models. Nature 415:626–630.

Hagen, S. C., B. H. Braswell, E. Linder, S. Frolking, A. D. Richardson, and D. Y. Hollinger. 2006. Statistical uncertainty of eddy flux-based estimates of gross ecosystem carbon exchange at Howland Forest, Maine. Journal of Geophysical Research: Atmospheres. doi: 10.1029/2005JD006154

He, L., J. M. Chen, Y. Pan, R. Birdsey, and J. Kattge. 2012. Relationships between net primary productivity and forest stand age in U.S. forests. Global Biogeochemical Cycles. doi: 10.1029/2010GB003942

Heinsch, F. A., et al. 2006. Evaluation of remote sensing based terrestrial productivity from MODIS using tower eddy flux network observations. IEEE Transactions on Geoscience and Remote Sensing 44:1908–1925.

Herbert, G. A., E. R. Green, J. M. Harris, G. L. Koenig, S. J. Roughton, and K. W. Thaut. 1986. Control and monitoring instrumentation for the continuous measurement of atmospheric CO_2 and meteorological variables. Journal of Atmospheric and Oceanic Technology 3:414–421.

Hoteit, I., G. Triantafyllou, G. Petihakis, and J. I. Allen. 2003. A singular evolutive extended Kalman filter to assimilate real in situ data in a 1-D marine ecosystem model. Annales Geophysicae 21:389–397.

Kalman, R. E. 1960. A new approach to linear filtering and prediction problems. Journal of Basic Engineering 82:35–45.

Kaminski, T., W. Knorr, P. Rayner, and M. Heimann. 2002. Assimilating atmospheric data into a terrestrial biosphere model: A case study of the seasonal cycle. Global Biogeochemical Cycles. doi: 10.1029/2001GB001463

Kaminski, T., M. Heimann, and R. Giering. 1999*a*. A coarse grid three-dimensional global inverse model of the atmospheric transport: 1. Adjoint model and Jacobian matrix. Journal of Geophysical Research: Atmospheres 104:18535–18553.

Kaminski, T., M. Heimann, and R. Giering. 1999*b*. A coarse grid three-dimensional global inverse model of the atmospheric transport: 2. Inversion of the transport of CO_2 in the 1980s. Journal of Geophysical Research: Atmospheres 104:18555–18581.

Kato, T., W. Knorr, M. Scholze, E. Veenendaal, T. Kaminski, J. Kattge, and N. Gobron. 2013. Simultaneous assimilation of satellite and eddy covariance data for improving terrestrial water and carbon simulations at a semi-arid woodland site in Botswana. Biogeosciences 10:789–802.

Kitajima, K., S. Mulkey, and S. Wright. 1997. Decline of photosynthetic capacity with leaf age in relation to leaf longevities for five tropical canopy tree species. American Journal of Botany 84:702–708.

Knorr, W., and J. Kattge. 2005. Inversion of terrestrial ecosystem model parameter values against eddy covariance measurements by Monte Carlo sampling. Global Change Biology 11:1333–1351.

Knyazikhin, Y., et al. 1999. MODIS leaf area index (LAI) and fraction of photosynthetically active radiation absorbed by vegetation (FPAR) product (MOD15) algorithm theoretical basis document. Theoretical Basis Document, NASA Goddard Space Flight Center, Greenbelt, Maryland, USA. http://modis.gsfc.nasa.gov/data/atbd/atbd_mod15.pdf

Komhyr, W. D., T. B. Harris, L. S. Waterman, J. F. S. Chin, and K. W. Thoning. 1989. Atmospheric carbon dioxide at Mauna Loa Observatory: 1. NOAA Global Monitoring for Climatic Change measurements with a nondispersive infrared ana-

lyzer, 1974-1985. Journal of Geophysical Research: Atmospheres 94:8533–8547.

Kuppel, S., P. Peylin, F. Chevallier, C. Bacour, F. Maignan, and A. D. Richardson. 2012. Constraining a global ecosystem model with multi-site eddy-covariance data. Biogeosciences 9:3317–3380.

Law, R. M., et al. 2008. TransCom model simulations of hourly atmospheric CO_2: Experimental overview and diurnal cycle results for 2002. Global Biogeochemical Cycles. doi: 10.1029/2007GB003050

Li, X., and C. Wunsch. 2004. An adjoint sensitivity study of chlorofluorocarbons in the North Atlantic. Journal of Geophysical Research: Oceans. doi: 10.1029/2003JC002014

Li, X., and C. Wunsch. 2003. Constraining the North Atlantic circulation between 4.5°S and 39.5°N with transient tracer observations. Journal of Geophysical Research: Oceans. doi: 10.1029/2002JC001765

Luo, Y., K. Ogle, C. Tucker, S. Fei, C. Gao, S. LaDeau, J. S. Clark, and D. S. Schimel. 2011. Ecological forecasting and data assimilation in a data-rich era. Ecological Applications 21:1429–1442.

Luo, Y., L. W. White, J. G. Canadell, E. H. DeLucia, D. S. Ellsworth, A. Finzi, J. Lichter, and W. H. Schlesinger. 2003. Sustainability of terrestrial carbon sequestration: a case study in Duke Forest with inversion approach. Global Biogeochemical Cycles. doi: 10.1029/2002GB001923

Marotzke, J., R. Giering, K. Q. Zhang, D. Stammer, C. Hill, and T. Lee. 1999. Construction of the Adjoint MIT Ocean General Circulation Model and Application to Atlantic Heat Transport Sensitivity. Journal of Geophysical Research: Oceans 104:29529–29547.

Masarie, K. A., R. L. Langenfelds, C. E. Allison, T. J. Conway, E. J. Dlugokencky, R. J. Francey, P. C. Novelli, L. P. Steele, P. P. Tans, B. Vaughn, and J. W. C. White. 2001. NOAA/CSIRO Flask Air Intercomparison Experiment: A strategy for directly assessing consistency among atmospheric measurements made by independent laboratories. Journal of Geophysical Research: Atmospheres 106:20445–20464.

Masarie, K. A., and P. P. Tans. 1995. Extension and integration of atmospheric carbon dioxide data into a globally consistent measurement record. Journal of Geophysical Research: Atmospheres 100:11593–11610.

McGuire, A. D., J. M. Melillo, L. A. Joyce, D. W. Kicklighter, A. L. Grace, B. Moore, III, and C. J. Vorosmarty. 1992. Interactions between carbon and nitrogen dynamics in estimating net primary productivity for potential vegetation in North America. Global Biogeochemical Cycles 6:101–124.

Melillo, J. M., A. D. McGuire, D. W. Kicklighter, B. Moore III, C. J. Vorosmarty, and A. L. Schloss. 1993. Global climate change and terrestrial net primary production. Nature 363:234–240.

Mitchell, T. D., T. R. Carter, P. D. Jones, M. Hulme, and M. New. 2004. A comprehensive set of high-resolution grids of monthly climate for Europe and the globe: the observed record (1901-2000) and 16 scenarios (2001-2100), climate scenarios for Europe and the globe, Tyndall Centre Working Paper 55. http://www.tyndall.ac.uk/sites/default/files/wp55.pdf

Mitchell, T. D., M. Hulme, and M. New. 2002. Climate data for political areas. Area 34:103–112.

Mo, X., J. M. Chen, W. Ju, and T. A. Black. 2008. Optimization of ecosystem model parameters through assimilating eddy covariance flux data with an ensemble Kalman filter. Ecological Modelling 217:157–173.

Monteith, J. L. 1972. Solar radiation and productivity in tropical ecosystems. Journal of Applied Ecology 9:747–766.

Mu, Q., M. Zhao, F. A. Heinsch, M. Liu, H. Tian, and S. W. Running. 2007. Evaluating water stress controls on primary production in biogeochemical and remote sensing based models, Journal of Geophysical Research: Biogeosciences. doi: 10.1029/2006JG000179

Nassar, R., et al. 2010. Modeling global atmospheric CO_2 with improved emission inventories and CO_2 production from the oxidation of other carbon species. Geoscientific Model Development 3:689–716.

Natvik, L. J., M. Eknes, and G. Evensen. 2000. A weak constraint inverse for a zero-dimensional marine ecosystem model. Journal of Marine Systems 28:19–44.

New, M., D. Lister, M. Hulme, and I. Makin. 2002. A high-resolution data set of surface climate over global land areas. Climate Research 21:1–25.

New, M., M. Hulme, and P. Jones. 2000. Representing twentieth century space-time climate variability. Part II: development of 1901-96 monthly grids of terrestrial surface climate. Journal of Climate 13:2217–2238.

New, M., M. Hulme, and P. Jones. 1999. Representing twentieth century space-time climate variability. Part I: development of a 1961-90 mean monthly terrestrial climatology. Journal of Climate 12:829–856.

Parton, W., J. Scurlock, D. Ojima, T. Gilmanov, R. Scholes, D. Schimel, T. Kirchner, J. Menaut, T. Seastedt, and E. G. Moya. 1993. Observations and modeling of biomass and soil organic matter dynamics for the grassland biome worldwide. Global Biogeochemical Cycles 7:785–809.

Potter, C. S., J. T. Randerson, C. B. Field, P. A. Matson, P. M. Vitousek, H. A. Mooney, and S. A. Klooster. 1993. Terrestrial ecosystem production: a process model based on global satellite and surface data.

Global Biogeochemical Cycles 7:811–841.

Pregitzer, K. S., and E. S. Euskirchen. 2004. Carbon cycling and storage in world forests: Biome patterns related to forest age. Global Change Biology 10:2052–2077.

Quaife, T., P. Lewis, M. De Kauwe, M. Williams, B. E. Law, M. Disney, and P. Bowyer. 2008. Assimilating canopy reflectance data into an ecosystem model with an Ensemble Kalman Filter. Remote Sensing of Environment 112:1347–1364.

Raich, J. W., E. B. Rastetter, J. M. Melillo, D. W. Kicklighter, P. A. Steudler, B. J. Peterson, A. L. Grace, B. Moore, III, and C. J. Vorosmarty. 1991. Potential net primary productivity in South America: Application of a global model. Ecological Applications 1:399–429.

Raupach, M. R., P. J. Rayner, D. J. Barrett, R. S. DeFries, M. Heimann, D. S. Ojima, S. Quegan, and C. C. Schmullius. 2005. Model-data synthesis in terrestrial carbon observation: methods, data requirements and data uncertainty specifications. Global Change Biology 11:378–397.

Rayner, R. J., M. Scholze, W. Knorr, T. Kaminski, R. Giering, and H. Widmann. 2005. Two decades of terrestrial carbon fluxes from a carbon cycle data assimilation system (CCDAS). Global Biogeochemical Cycles. doi: 10.1029/2004GB002254

Reichle, R. H., D. B. McLaughlin, and D. Entekhabi. 2002. Hydrologic data assimilation with the ensemble Kalman filter. Monthly Weather Review 130:103–114.

Reichstein, M., et al. 2005. On the separation of net ecosystem exchange into assimilation and ecosystem respiration: review and improved algorithm. Global Change Biology 11:1424–1439.

Ricciuto, D. M., K. J. Davis, and K. Keller. 2008*a*. A Bayesian calibration of a simple carbon cycle model: The role of observations in estimating and reducing uncertainty. Global Biogeochemical Cycles. doi: 10.1029/2006GB002908

Ricciuto, D. M., M. P. Butler, K. J. Davis, B. D. Cook, P. S. Bakwin, A. Andrews, and R. M. Teclaw. 2008*b*. Causes of interannual variability in ecosystem-atmosphere CO_2 exchange in a northern Wisconsin forest using a Bayesian model calibration. Agricultural and Forest Meteorology 148:309–327.

Richardson, A. D., et al. 2006. A multi-site analysis of random error in tower-based measurements of carbon and energy fluxes. Agricultural and Forest Meteorology 136:1–18.

Rounsevell, M. D. A., J. E. Annetts, E. Audsley, T. Mayr, and I. Reginster. 2003. Modeling the spatial distribution of agricultural land use at the regional scale. Agriculture Ecosystems & Environment 95:465–479.

Running, S. W., R. R. Nemani, F. A. Heinsch, M. Zhao, M. Reeves, and H. Hashimoto. 2004. A continuous satellite-derived measure of global terrestrial primary productivity: Future science and applications. BioScience 54:547–560.

Running, S. W., and J. C. Coughlan. 1988. A general model of forest ecosystem processes for regional applications I. Hydrologic balance, canopy gas exchange and primary production processes. Ecological Modelling 42:125–154.

Schartau, M., A. Oschlies, and J. Willebrand. 1999. Parameter estimates of a zero-dimensional ecosystem model applying the adjoint method. Deep Sea Research Part II: Topical Studies in Oceanography 48:1769–1800.

Schmid, H. P. 1994. Source areas for scalars and scalar fluxes. Boundary-Layer Meteorology 67:293–318.

Scholze, M., T. Kaminski, P. Rayner, W. Knorr, and R. Giering. 2007. Propagating uncertainty through prognostic carbon cycle data assimilation system simulations. Journal of Geophysical Research: Atmospheres. doi: 10.1029/2007JD008642

Senina, I., J. Sibert, and P. Lehodey. 2008. Parameter estimation for basin-scale ecosystem-linked population models of large pelagic predators: Application to skipjack tuna. Progress in Oceanography 78:319–335.

Staniforth, A., and J. Cote. 1991. Semi-Lagrangian integration schemes for atmospheric models-a review. Monthly Weather Review 119:2206–2223.

Sulman, B. N., A. R. Desai, B. D. Cook, N. Saliendra, and D. S. Mackay. 2009. Contrasting carbon dioxide fluxes between a drying shrub wetland in Northern Wisconsin, USA, and nearby forests. Biogeosciences 6:1115–1126.

Suntharalingam, P., J. T. Randerson, N. Krakauer, J. A. Logan, and D. J. Jacob. 2005. Influence of reduced carbon emissions and oxidation on the distribution of atmospheric CO_2: Implications for inversion analyses. Global Biogeochemical Cycles. doi: 10.1029/2005GB002466

Suntharalingam, P., D. J. Jacob, P. I. Palmer, J. A. Logan, R. M. Yantosca, Y. Xiao, M. J. Evans, D. G. Streets, S. L. Vay, and G. W. Sachse. 2004. Improved quantification of Chinese carbon fluxes using CO_2/CO correlations in Asian outflow. Journal of Geophysical Research: Atmospheres. doi: 10.1029/2003JD004362

Suntharalingam, P., C. Spivakovsky, J. Logan, and M. McElroy. 2003. Estimating the distribution of terrestrial CO_2 sources and sinks from atmospheric measurements: Sensitivity to configuration of the observation network. Journal of Geophysical Research: Atmospheres. doi: 10.1029/2002JD002207

Takahashi, T., et al. 2009. Climatological mean and decadal change in surface ocean PCO_2, and net met sea-air CO_2 flux over the global oceans. Deep Sea Research Part II: Topical Studies in Oceanography 56:554–577.

Tang, J., and Q. Zhuang. 2009. A global sensitivity analysis and Bayesian inference framework for improving the parameter estimation and prediction of a process-based Terrestrial Ecosystem Model. Journal of Geophysical Research: Atmospheres. doi: 10.1029/2009JD011724

Tang, J., and Q. Zhuang. 2008. Equifinality in parameterization of process-based biogeochemistry models: A significant uncertainty source to the estimation of regional carbon dynamics. Journal of Geophysical Research: Biogeosciences. doi: 10.1029/2008JG000757

Tarantola, A. 1987. Inverse problem theory: methods for data fitting and parameter estimation. Elsevier, New York, New York, USA.

Thoning, K. W. 1989. Selection of NOAA/GMCC CO_2 data from Mauna Loa Observatory. Pages 1–13 *in* W. P. Elliott, editor. The statistical treatment of CO_2 data records. NOAA Technical Memorandum ERL ARL-173. Air Resources Laboratory, Silver Spring, Maryland, USA.

Tjiputra, J. F., and A. M. E. Winguth. 2008. Sensitivity of sea-to-air CO_2 flux to ecosystem parameters from an adjoint model. Biogeosciences 5:615–630.

Tjiputra, J. F., D. Polzin, and A. M. E. Winguth. 2007. Assimilation of seasonal chlorophyll and nutrient data into an adjoint three-dimensional ocean carbon cycle model: Sensitivity analysis and ecosystem parameter optimization. Global Biogeochemical Cycles. doi: 10.1029/2006GB002745

Urbanski, S., C. Barford, S. Wofsy, C. Kucharik, E. Pyle, J. Budney, K. McKain, D. Fitzjarrald, M. Czikowsky, and J. W. Munger. 2007. Factors Controlling CO_2 exchange on time scales from hourly to decadal at Harvard Forest. Journal of Geophysical Research: Biogeosciences. doi: 10.1029/2006JG000293

van der Werf, G. R., J. T. Randerson, L. Giglio, G. J. Collatz, P. S. Kasibhatla, and A. F. Arellano, Jr. 2006. Interannual variability in global biomass burning emissions from 1997-2004. Atmospheric Chemistry and Physics 6:3423–3441.

van Gorsel, E., et al. 2009. Estimating nocturnal ecosystem respiration from vertical turbulent flux and change in storage CO_2. Agricultural and Forest Meteorology 149:1919–1930.

Wang, W., K. Ichii, H. Hashimoto, A. Michaelis, P. Thornton, B. Law, and R. Nemani. 2009. A hierarchical analysis of the terrestrial ecosystem model BIOME-BGC: model calibration and equilibrium analysis. Ecological Modelling 220:2009–2023.

Xu, T., L. White, D. Hui, and Y. Luo. 2006. Probabilistic inversion of a terrestrial ecosystem model: Analysis of uncertainty in parameter estimation and model prediction. Global Biogeochemical Cycles. doi: 10.1029/2005GB002468

Yevich, R., and J. A. Logan. 2003. An assessment of biofuel use and burning of agricultural waste in the developing world. Global Biogeochemical Cycles. doi: 10.1029/2002GB001952

Yuan, W., et al. 2007. Deriving a light use efficiency model for eddy covariance flux data for predicting daily gross primary production across biomes. Agricultural and Forest Meteorology 143:189–207.

Zaehle, S., S. Sitch, C. Prentice, J. Liski, W. Cramer, M. Erhard, T. Hickler, and B. Smith. 2006. The importance of age-related decline in forest NPP for modeling regional carbon balances. Ecological Applications 16:1555–1574.

Zaehle, S., S. Sitch, B. Smith, and F. Hatterman. 2005. Effects of parameter uncertainties on the modeling of terrestrial biosphere dynamics. Global Biogeochemical Cycles. doi: 10.1029/2004GB002395

Zhang, G. J., and N. A. McFarlane. 1995. Sensitivity of climate simulations to the parameterization of cumulus convection in the Canadian Climate Centre general circulation model. Atmosphere-Ocean 33:407–446.

Zhao, M., S. W. Running, and R. R. Nemani. 2006. Sensitivity of Moderate Resolution Imaging Spectroradiometer (MODIS) terrestrial primary production to the accuracy of meteorological reanalyses. Journal of Geophysical Research: Biogeosciences. doi: 10.1029/2004JG000004

Zhao, M., F. A. Heinsch, R. R. Nemani, and S. W. Running. 2005. Improvements of the MODIS terrestrial gross and net primary production global dataset. Remote Sensing of Environment 95:164–176.

Zhou, T., P. Shi, D. Hui, and Y. Luo. 2009. Global pattern of temperature sensitivity of soil heterotrophic respiration (Q_{10}) and its implications for carbon-climate feedback. Journal of Geophysical Research: Biogeosciences. doi: 10.1029/2008JG000850

Zhou, T., and Y. Luo. 2008. Spatial patterns of ecosystem carbon residence time and NPP-driven carbon uptake in the conterminous United States. Global Biogeochemical Cycles doi: 10.1029/2007GB002939

Zhou, X., T. Zhou, and Y. Luo. 2012. Uncertainties in carbon residence time and NPP-driven carbon uptake in terrestrial ecosystems of the conterminous USA: a Bayesian approach. Tellus B. doi: 10.3402/tellusb.v64i0.17223

Zhuang, Q., A. D. McGuire, J. M. Melillo, J. S. Clein, R. J. Dargaville, D. W. Kicklighter, R. B. Myneni, J. Dong, V. E. Romanovsky, J. Harden, and J. E. Hobbie. 2003. Carbon cycling in extratropical terrestrial ecosystems of the Northern Hemisphere during the 20th century: a modeling analysis of the influences of soil thermal dynamics. Tellus B 55:751–767.

Zhuang, Q., A. D. McGuire, K. P. O'Neil, J. Harden, V. E. Romanovsky, and J. Yarie. 2002. Modeling the soil thermal and carbon dynamics of a fire chronosequence in interior Alaska. Journal of Geophysical Research: Atmospheres. doi: 10.1029/2001JD001244

Zhuang, Q., V. E. Romanovsky, and A. D. McGuire. 2001. Incorporation of a permafrost model into a large-scale ecosystem model: Evaluation of temporal and spatial scaling issues in simulating soil thermal dynamics. Journal of Geophysical Research: Atmospheres 106:33649–33670.